
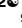






RESEARCH ARTICLE

Retinoid orphan receptor gamma t (rorγt) promotes inflammatory eosinophilia but is dispensable for innate immune-mediated colitis

Alvaro Torres-Huerta¹ , Katelyn Ruley-Haase² , Theodore Reed² , Antonia Boger-May¹, Derek Rubadeux² , Lauren Mayer², Arpitha Mysore Rajashekara², Morgan Hiller², Madeleine Frech², Connor Roncagli² , Cameron Pedersen², Mary Catherine Camacho², Lauren Hollmer², Lauren English², Grace Kane², David L. Boone^{1,2*} 

1 Department of Microbiology & Immunology, Indiana University School of Medicine-South Bend, South Bend, IN, United States of America, **2** Department of Biology, University of Notre Dame, South Bend, IN, United States of America

 These authors contributed equally to this work.

* dboone@nd.edu



OPEN ACCESS

Citation: Torres-Huerta A, Ruley-Haase K, Reed T, Boger-May A, Rubadeux D, Mayer L, et al. (2024) Retinoid orphan receptor gamma t (rorγt) promotes inflammatory eosinophilia but is dispensable for innate immune-mediated colitis. PLoS ONE 19(3): e0300892. <https://doi.org/10.1371/journal.pone.0300892>

Editor: Masanori A. Murayama, Kansai Medical University: Kansai Ika Daigaku, Institute of Biomedical Science, JAPAN

Received: October 6, 2023

Accepted: March 5, 2024

Published: March 21, 2024

Copyright: © 2024 Torres-Huerta et al. This is an open access article distributed under the terms of the [Creative Commons Attribution License](https://creativecommons.org/licenses/by/4.0/), which permits unrestricted use, distribution, and reproduction in any medium, provided the original author and source are credited.

Data Availability Statement: All relevant data are within the manuscript and its [Supporting Information](#) files.

Funding: Supported by funding from the National Institute for Diabetes and Digestive and Kidney (NIH) to David Boone (R01DK120320), and from the American Gastroenterology Association to David Boone. This project was funded with support from the Indiana Clinical and Translational Sciences

Abstract

Inflammatory bowel diseases (IBD) result from uncontrolled inflammation in the intestinal mucosa leading to damage and loss of function. Both innate and adaptive immunity contribute to the inflammation of IBD and innate and adaptive immune cells reciprocally activate each other in a forward feedback loop. In order to better understand innate immune contributions to IBD, we developed a model of spontaneous 100% penetrant, early onset colitis that occurs in the absence of adaptive immunity by crossing villin-TNFAIP3 mice to RAG1^{-/-} mice (TRAG mice). This model is driven by microbes and features increased levels of innate lymphoid cells in the intestinal mucosa. To investigate the role of type 3 innate lymphoid cells (ILC3) in the innate colitis of TRAG mice, we crossed them to retinoid orphan receptor gamma t deficient (Rorγt^{-/-}) mice. Rorγt^{-/-} x TRAG mice exhibited markedly reduced eosinophilia in the colonic mucosa, but colitis persisted in these mice. Colitis in Rorγt^{-/-} x TRAG mice was characterized by increased infiltration of the intestinal mucosa by neutrophils, inflammatory monocytes, macrophages and other innate cells. RNA and cellular profiles of Rorγt^{-/-} x TRAG mice were consistent with a lack of ILC3 and ILC3 derived cytokines, reduced antimicrobial factors, increased activation of epithelial repair processes and reduced activation of epithelial cell STAT3. The colitis in Rorγt^{-/-} x TRAG mice was ameliorated by antibiotic treatment indicating that microbes contribute to the ILC3-independent colitis of these mice. Together, these gene expression and cell signaling signatures reflect the double-edged sword of ILC3 in the intestine, inducing both proinflammatory and antimicrobial protective responses. Thus, Rorγt promotes eosinophilia but Rorγt and Rorγt-dependent ILC3 are dispensable for the innate colitis in TRAG mice.

Institute which is funded in part by Award Number UM1TR004402 from the National Institutes of Health, National Center for Advancing Translational Sciences, Clinical and Translational Sciences Award.

Competing interests: The authors have declared that no competing interests exist.

Introduction

Inflammatory bowel diseases (Crohn's disease and ulcerative colitis) are characterized by damaging chronic inflammation in the gastrointestinal tract. The causes of inflammatory bowel diseases (IBD) are not known but a current paradigm is that genetics and environment contribute to susceptibility to disease [1, 2]. The environmental factors that contribute to IBD are not known but it is likely that these factors manifest, at least in part, through changes in the gut microbiome. A key component of host interactions with the microbial world is the innate immune system and so innate immunity is considered central to the pathogenesis of IBD [3].

Both innate and adaptive immunity contribute to IBD. Innate cells detect microbes and initiate the immune response, leading to activation and expansion of antigen specific adaptive immune cells. The adaptive responses produce cytokines that subsequently activate innate defenses, which can further induce adaptive immune cells in a positive feedback loop. This reciprocal interaction between innate and adaptive immunity creates the inflammation needed to defend against pathogens, but in pathological states like IBD the inflammation persists and damages the gut tissue leading to loss of function and IBD. A better understanding the causes of IBD requires more complete information about the nature of both the adaptive and innate immune pathology. However, the reciprocal nature of the adaptive and innate feedback loop makes it challenging to identify innate mechanisms that lead to IBD. Innate models of IBD that occur in the absence of adaptive immunity can address this challenge and provide insight into innate mechanisms of inflammation [4–6]. For example, a key role for type 3 innate lymphoid cells in IBD was revealed by studies using innate models of IBD lacking the transcription factor retinoid orphan receptor gamma t (RoRyt) [5]. Thus, models of IBD that occur in the absence adaptive immunity can provide valuable insight into innate immune mechanisms of disease.

We have developed a unique innate immune model of IBD that occurs spontaneously with 100% penetrance at 6 weeks-of-age in C57Bl/6 mice [6, 7]. Transgenic mice expressing tumor necrosis factor induced protein 3 (TNFAIP3; aka A20) in intestinal epithelial cells under the villin promoter (v-TNFAIP3) develop colitis on the recombination activating 1 (RAG1) deficient background (v-TNFAIP3 x RAG1^{-/-}) [6]. The mucosal inflammation in v-TNFAIP3 x RAG1^{-/-} (TRAG) mice is evident as increased innate immune infiltration in the colon by 4 weeks of age and histologically by 6 to 8 weeks of age [6]. Antibiotics prevent colitis in TRAG mice, indicating that microbes drive the colitis in this innate model [6]. The expression of TNFAIP3 in the intestinal epithelium leads to altered microbial biogeography with invasion of the inner mucus layer by microbes, predominantly of the class Actinobacteria and Gammaproteobacteria [7, 8]. Despite this microbial invasion, v-TNFAIP3 mice do not develop colitis [7–9]. RAG1^{-/-} mice maintain an inner mucus layer largely devoid of microbes and also do not develop colitis [7]. However, 100% of TRAG mice develop colitis indicating that a combination of microbial invasion of the inner mucus layer and immunodeficiency leads to innate immune colitis. We found that treatment of TRAG mice with anti-Thy1.2 antibody to deplete innate lymphoid cells (ILC) could both prevent or reverse established colitis [6]. However, unlike other innate models of IBD, crossing TRAG mice to mice lacking RoRyt did not prevent colitis [6]. Thus, colitis in TRAG mice likely involves unique innate immune mechanisms and so herein we provide a more detailed characterization of the colitis that occurs in TRAG mice in the absence of RoRyt.

Materials and methods

Animal studies

Mice were bred and housed in the Freimann Life Sciences Center at the University of Notre Dame (protocol#23-03-7746). No anesthesia or analgesia was performed. Euthanasia was

performed by carbon dioxide asphyxiation with secondary cervical dislocation. All protocols were performed at the University of Notre Dame Freimann Life Science Center approved by Institutional Animal Care and Use Committees. All mice were bred and maintained on the C57BL/6 background. The villin-TNFAIP3 strain was generated previously using BAC-recombineering of the villin locus and characterized as described [9]. $RAG1^{-/-}$ and $Rorc^{-/-}$ mice (C57BL/6) were purchased from Jackson Laboratories and interbred to villin-TNFAIP3 mice to generate villin-TNFAIP3 \times $RAG1^{-/-}$ (TRAG) mice, $Rorc^{-/-}$ \times TRAG mice, or $RAG1^{-/-}$ littermate controls.

RNA extraction and RNAseq analysis

Colonic mucosal tissues were harvested by transecting the colon, washing out contents in ice cold PBS, and scraping mucosa using a glass slide to separate it from the underlying muscle layer. Tissues were harvested and immediately frozen in liquid nitrogen and stored at -80°C . RNA was extracted using TRIzol reagent (Thermo Fisher) as per the manufacturer protocol and stored at -80°C . Preparation of RNA library and transcriptome sequencing was conducted by Novogene Co., LTD (Sacramento, CA).

Analysis of RNAseq was performed according to the methods provided by Novogene as follows (text provided by Novogene): “Raw data (raw reads) of fastq format were firstly processed through in-house perl scripts. In this step, clean data (clean reads) were obtained by removing reads containing adapter, reads containing ploy-N and low-quality reads from raw data. At the same time, Q20, Q30, and GC content the clean data were calculated. All the downstream analyses were based on the clean data with high quality.

Reference genome and gene model annotation files were downloaded from genome website directly. Index of the reference genome was built using Hisat2 v2.0.5 and paired-end clean reads were aligned to the reference genome using Hisat2 v2.0.5. We selected Hisat2 as the mapping tool for that Hisat2 can generate a database of splice junctions based on the gene model annotation file and thus a better mapping result than other non-splice mapping tools.

featureCounts v1.5.0-p3 was used to count the reads numbers mapped to each gene. And then FPKM of each gene was calculated based on the length of the gene and reads count mapped to this gene. FPKM, expected number of Fragments Per Kilobase of transcript sequence per Millions base pairs sequenced, considers the effect of sequencing depth and gene length for the reads count at the same time, and is currently the most commonly used method for estimating gene expression levels.

Differential expression analysis of two conditions/groups (two biological replicates per condition) was performed using the DESeq2 R package (1.20.0). DESeq2 provides statistical routines for determining differential expression in digital gene expression data using a model based on the negative binomial distribution. The resulting P-values were adjusted using the Benjamini and Hochberg’s approach for controlling the false discovery rate. Genes with an adjusted P-value ≤ 0.05 found by DESeq2 were assigned as differentially expressed.”

Histology scoring

Mouse intestinal tissues were fixed in Methyl Carnoy’s, processed and embedded in paraffin and sectioned at $5\mu\text{M}$. Sections were stained by H&E and then scored for histopathology of colitis using methods previously described [10]. Briefly, eight criteria were assessed on a scale of 0–3 to determine the severity of colitis: infiltrate, goblet cell loss, crypt density, crypt hyperplasia, muscle thickening, submucosal infiltrate, and presence of ulceration or abscesses to produce a score ranging from 0 to 24. Each category was assessed with the following criteria: Infiltrate: 0-none, 1-increased presence of inflammatory cells, 2-infiltrates also in submucosa, 3- transmural. Goblet cell loss: 0-none, 1- $<10\%$, 2- $10\text{--}50\%$, 3- $>50\%$. Crypt density: 0-

normal, 1-decreased by <10%, 2- decreased by 10–50%, 3-decreased by >50%. Crypt hyperplasia: 0-none, 1- slight increase in crypt length, 2–2 to 3-fold increase in crypt length, 3- three-fold increase in crypt length. Muscle thickening: 0-none, 1-slight, 2-strong, 3- excessive. Submucosal inflammation: 0-none, 1-individual cells, 2-infiltrate, 3- large infiltrates. Crypt Abscess and ulceration was either absent (0) or present (3).

Immunofluorescence

Methyl Carnoys fixed tissues were processed and sectioned as described above. Following rehydration to PBS, antigen retrieval was performed by boiling in sodium citrate buffer pH6 for 10 minutes followed by 20 minutes cooling, washing in TBS and blocking in TBS + 0.05% Tween-20 (TBST) containing 1% BSA and 5% donkey serum (1hr, RT). Sections were then stained with antibodies to EPCAM and phosphorylated STAT3 in TBST+1% BSA+5%donkey serum (4C, overnight), washed in TBST (3X 5min), incubated in secondary antibodies (1hr, RT), washed in TBST (3 X 5min) and mounted in Prolong Gold media with DAPI. Fluorescent images were acquired on a Leica DM5500 fluorescence microscope. To quantify the number of phospho-STAT3 positive intestinal epithelial cells, three images from representative regions (proximal or distal colon) of three mice were counted. The number of DAPI positive and phospho-STAT3 positive epithelial cells in 3–4 crypts was acquired and the data were normalized to represent the number of phospho-STAT3 positive cells per 100 epithelial cells.

Lamina Propria Leukocytes (LPL) isolation

LPL were isolated from colons as described [11]. Colons along with cecum (without cecal lymphoid patch) were excised, thoroughly cleared of fecal content and residual fat, cut longitudinally, and diced. The sections were washed with several rounds of calcium-magnesium free media with (2%) serum (CMF) to remove feces and mucus. Tissue pieces were shaken at 37°C in CMF with 1mM dithioerythritol (DTE) and 2mM EDTA twice for 20 minutes with agitation after each incubation. Tissue pieces were then rinsed with RPMI and subsequently shaken for ~1 hour with 100U/ml collagenase (Sigma) and 10U/ml DNase (Sigma) in RPMI with agitation every 20 minutes. Digested tissue sections were then passed through a 70µm filter to eliminate large tissue and collect dissociated cells. Cells were washed in RPMI and centrifuged at 300 xg for 10 minutes. Percoll (40% in RPMI) was then added to cell pellets and centrifuged at 600xg, RT for 20 minutes. Percoll was removed and the cell pellet collected, washed in RPMI, and used for flow cytometry analysis.

Flow cytometry

Colon LPLs were suspended in FACS buffer (2%FBS in PBS) and incubated with Fc Block antibody (10min on ice) followed by viability dye eFlour-780 for 30 minutes at 4°C to identify non-viable cells. Cells were then washed with FACS buffer and incubated with antibodies (Table 1) for 30 minutes at 4°C, washed with FACS buffer and fixed with paraformaldehyde (PFA) (1% PFA in PBS). The fluorescence of individual cells was evaluated through the sample acquisition in a BD LRS-Fortessa X-20 cytometer, analyzed with flow Jo v10.7 and dimensional 2D reduction performed using UMAP [12].

The following markers used to distinguish immune cell subsets (all CD45+ve cells) are listed in Table 2 below.

Antibiotic treatments

Mice, beginning at 4 weeks of age, were fed a cocktail of four antibiotics, or control water, as described [7]. Ampicillin (0.5g/ml), Neomycin (0.25g/ml), Metranidazole (62.5mg/ml) and

Table 1. List of antibodies, fluorophores and reagents used in flow cytometry.

Antibody to:	Fluorophore	Company	Identifier
CD16/CD32 (FcBlock)	N/A	BD Biosciences	553142
Viability Dye	eFlour-780	Thermo Fisher	65-0865-14
CD45	BV711	BioLegend	103147
CD11b	APC-R700	BD Biosciences	564985
CD11c	PE-Cy7	Thermo Fisher	25-0114-81
MHCII	PE	BioLegend	107607
Thy1.2	FITC	Thermo Fisher	11-0903-82
SiglecF	eFlour-660	Thermo Fisher	50-1702-80
Ly6G	BV650	BioLegend	127641
Ly6C	BV421	BD Biosciences	562727
NK1.1	BV785	Thermo Fisher	108749
F4/80	PE-Cy5	Thermo Fisher	15-4801-80
CompBeads anti-Rat and Anti-Hamster Igk		BD Biosciences	552845
CompBeads anti-Mouse Igk		BD Biosciences	552843

<https://doi.org/10.1371/journal.pone.0300892.t001>

Vancomycin (125mg/ml) were provided as a cocktail dissolved in grape KoolAid. Control mice received KoolAid only. Antibiotics were refreshed twice weekly until the mice were 8 weeks of age when colon tissues were collected for histology.

Statistical analysis and reagents

Bar graphs represent the mean plus standard deviation of each group with individual data points representing data from one mouse. Male and female mice were grouped together as there were no significant gender-based differences in the data. Data were analyzed by one way ANOVA with post hoc non-parametric tests for histological scoring (Kruskal-Wallis and Dunn's multiple comparison) or post-hoc Tukey's tests for LPL cell counts. Statistical analysis of RNAseq data was performed as described in the Section for RNAseq analysis. Significance was inferred at a p value less than 0.05. All reagents used in these studies are indicated in [Table 3](#).

Results

TRAG mice develop 100% penetrant, early onset colitis in the absence of adaptive antigen receptor expressing cells [6, 7]. We have observed that TRAG mice can develop colitis in the absence of RoR γ t, the transcription factor required for ILC3 development [6, 13]. To better characterize and quantify the role of RoR γ t in the histopathological features of colitis in TRAG

Table 2. Markers that define individual cell subtypes in the gut lamina propria.

CD45 gate	Positive Markers	Negative Markers
Neutrophils	Ly6G, CD11b	
Monocytes	Ly6C, CD11b	MHCII
Inflammatory monocytes	Ly6C, CD11b, MHCII	
Macrophages	F4/80, MHCII, CD11b	CD11c
Eosinophils	SiglecF, CD11b	
Dendritic Cells	CD11c, MHCII	CD11b
Natural Killers	NK1.1, CD11b ^{medium}	
Innate Lymphoid Cells	Thy1	CD11b

<https://doi.org/10.1371/journal.pone.0300892.t002>

Table 3. List of reagents.

Reagent	Source	Identifier
Vancomycin Hydrochloride from <i>Streptomyces orientalis</i>	Sigma-Aldrich	94747
Metronidazole	Sigma-Aldrich	M1547
Neomycin Sulfate	Fisher Scientific	BP2669-5
Ampicillin Sodium	Fisher Scientific	BP1760
Kool-Aid Soft Drink Mix Grape Unsweetened, Caffeine Free—3.9g	Walmart Inc.	Barcode# 4300 95563
Great Value Granulated No Calorie Sweetener Value Pack, 19.4 oz	Walmart Inc.	Barcode# 28742 04883
Percoll	Cytiva	17089101
RPMI	Cytiva	SH30011.04
1,4-Dithioerythritol, 98+%	Thermo Fisher	A10138.06
Ethylenediamine Tetraacetate (EDTA)	Fisher Scientific	BP2483500
HBSS 10X	Thermo Fisher	14185052
Sodium Phosphate Dibasic Anhydrous	Fisher Scientific	S374-500
Potassium Chloride, Enzyme Grade	Fisher Scientific	BP366-500
Potassium Phosphate Dibasic	Fisher Scientific	BP362-1
Sodium chloride, crystalline powder PDV, 99+%	Thermo Fisher	A12313
HyClone Iron-Supplemented calf Serum	Cytiva	SH30072.03
Collagenase Type I	Thermo Fisher	17100-017
Deoxyribonuclease I from bovine pancreas	Sigma	DN25-1G
CompBeads anti-Rat and Anti-Hamster Igκ	BD Biosciences	552845
CompBeads anti-Mouse Igκ	BD Biosciences	552843
ProLong TM Gold Antifade Mountaint with DNA stain DAPI	Thermo Fisher	P36935
Sodium Citrate Dihydrate	Fisher Scientific	BP327-1
TWEEN [®] 20	Millipore Sigma	9005-64-5
Bovine Serum Albumin	Fisher Scientific	NC1066518
Epcam Alexa Flour 647	Biologend	118212
pSTAT3	CST	9145S
Donkey anti-Rabbit IgG (H+L) Alexa Flour 488	Thermo Fisher	A21206
Donkey serum	Millipore Sigma	D9663-10ML

<https://doi.org/10.1371/journal.pone.0300892.t003>

mice, we applied an 8 point histological scoring system [10] comparing RAG1^{-/-}, TRAG and Rorc^{-/-} x TRAG histopathology along the proximal to distal axis of the colon. We have observed distinct biogeographic distributions of microbes along the proximal to distal axis of the colon in TRAG mice and these can impact the severity of colitis and immune profiles, and so we assessed colitis severity in the cecum, proximal colon and distal colon independently [7]. Consistent with prior results, TRAG mice exhibited significantly higher histological scores of colitis compared to RAG1^{-/-} mice, in the cecum, proximal and distal colon (Fig 1). This colitis was also significantly increased in Rorc^{-/-} x TRAG mice, compared to RAG1^{-/-} mice (Fig 1). However, there was a trend toward lower histological scores, which was statistically significant, in the distal colon, of Rorc^{-/-} x TRAG mice, compared to TRAG mice (Fig 1). Thus, the absence of RoRyt ameliorates but does not prevent colitis in TRAG mice.

To assess the cellular innate immune profile of RoRyt-deficient TRAG mice we examined the LPL populations of these mice at 8 weeks of age (Fig 2). Rorc^{-/-} x TRAG mice showed significantly increased numbers of CD45^{+ve} leukocytes in the intestinal mucosa, compared to RAG1^{-/-} mice, and the number of these CD45 leukocytes was comparable between TRAG and Rorc^{-/-} x TRAG mice. Most innate immune cell populations were significantly increased in Rorc^{-/-} x TRAG mice compared to RAG1^{-/-} mice, and were similar in number to those of TRAG mice (Fig 2). One notable exception was that Rorc^{-/-} x TRAG mice had significantly

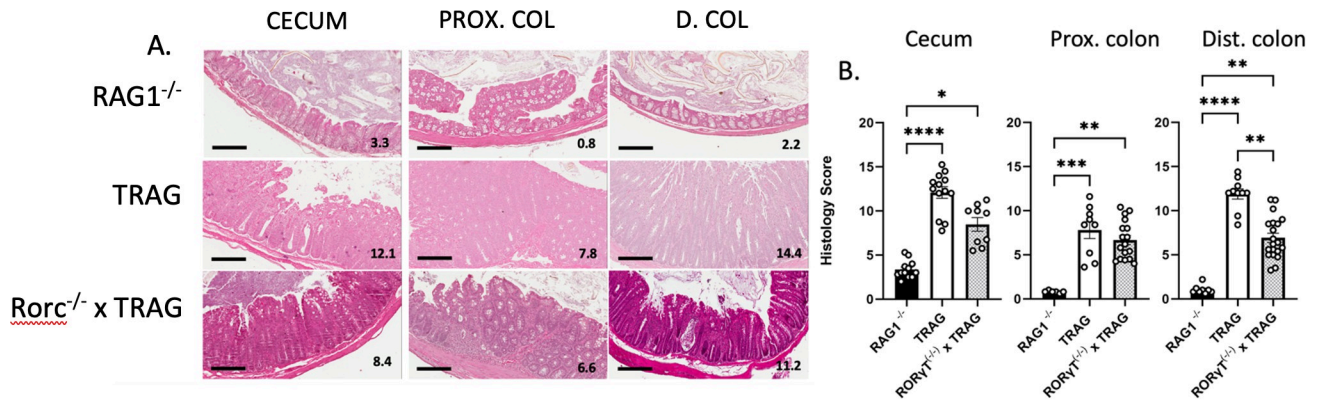


Fig 1. RoRyt is dispensable for colitis in TRAG mice. (A) Representative H&E sections of the cecum, proximal colon (PROX.COL) and distal colon (D. COL) of 8-week-old RAG1^{-/-}, TRAG and Rorc^{-/-} x TRAG mice. scale bar = 200μM. inset numbers are the scores for each section. (B) Histological scores of the cecum, proximal colon and distal colon. Each data point represents one mouse. *p<0.05, **p<0.01, ***p<0.005, ****p<0.001.

<https://doi.org/10.1371/journal.pone.0300892.g001>

fewer eosinophils than TRAG mice. There were also decreased numbers of neutrophils and ILCs in Rorc^{-/-} x TRAG vs. TRAG mice. This likely reflects the lack of ILC3 in Rorc^{-/-} x TRAG mice and the lack of granulocyte stimulation due the absence of ILC3-derived IL17. Thus, RoRyt^{+ve} cells contribute to the colitis in TRAG mice, especially toward the number of eosinophils in the intestinal mucosa, but RoRyt^{+ve} cells are nonetheless dispensable for colitis in this innate model.

To understand the molecular features of colitis in Rorc^{-/-} x TRAG mice, we performed RNAseq of TRAG and Rorc^{-/-} x TRAG colonic mucosal scrapings. TRAG and Rorc^{-/-} x TRAG colons had 451 and 586 uniquely expressed genes, respectively, and 12064 genes were expressed in both genotypes (Fig 3). There were 1876 differentially expressed genes, with 972 increased in expression in TRAG vs. Rorc^{-/-} x TRAG mice, and 904 genes exhibiting decreased expression. GO enrichment analysis indicated that biological processes were enriched for neutrophil and leukocyte chemotaxis and regulation of inflammation in TRAG vs. Rorc^{-/-} x TRAG mice (Fig 3). Molecular functions enriched in TRAG vs. Rorc^{-/-} x TRAG mice included cytokine and chemokine signaling. KEGG enrichment analysis of TRAG vs. Rorc^{-/-} x TRAG mucosa found that cytokine-receptor, IL17 signaling, and inflammatory bowel disease were the most significantly enriched pathways (Fig 3). Other enriched pathways included TNF signaling and NfκappaB signaling. Similarly, the reactome enrichment analysis comparing TRAG vs. Rorc^{-/-} x TRAG implicated cytokine signaling and neutrophil degranulation but also antimicrobial peptides and IL-6 family signaling (Fig 3). Together these transcriptome results are consistent with reduced colitis observed in the histopathology of Rorc^{-/-} x TRAG mice, compared to TRAG mice, and especially to the reduced granulocyte populations in Rorc^{-/-} x TRAG intestinal mucosa.

RoRyt expressing ILC3 produce IL17 and IL22, both of which can contribute to eosinophilia and granulocyte recruitment, which may explain the reduced the reduced numbers of granulocytes in the mucosa of Rorc^{-/-} x TRAG mice compared to TRAG mice [14, 15]. In addition, expression of other eosinophil activating cytokines like IL33 and IL36a [16–19] were reduced in Rorc^{-/-} x TRAG colons (Fig 4). Lastly, expression of chemokines that are produced by activated eosinophils, including cxcl1 and cxcl5 [16, 20] were reduced in Rorc^{-/-} x TRAG colons, consistent with the significant reduction of eosinophil numbers in the mucosa of Rorc^{-/-} x TRAG mice (Figs 2 and 4). The reduced expression of cytokines that induce eosinophilia and the reduced expression of cytokines made by activated eosinophils is consistent

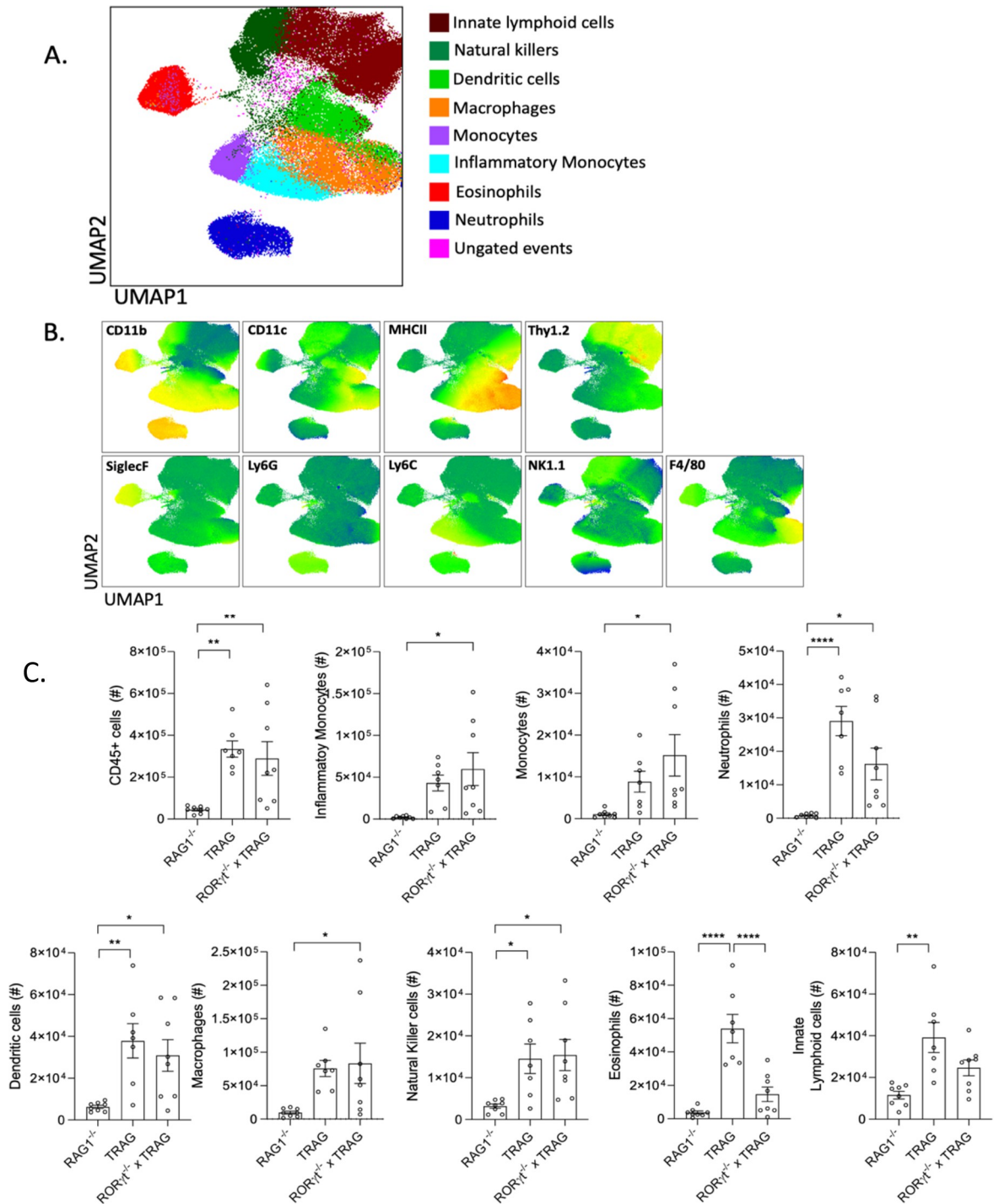


Fig 2. Immune profile of TRAG mice lacking RoRyt. (A,B) UMAP plots with markers of immune cell populations isolated from the lamina propria of 8-week-old RAG1^{-/-}, TRAG and Rorc^{-/-} x TRAG mice. (C) Cell counts from LPL preparations of 8-week-old RAG1^{-/-}, TRAG and Rorc^{-/-} x TRAG mice. Each data point represents one mouse. *p<0.05, **p<0.01, ***p<0.005, ****p<0.001.

<https://doi.org/10.1371/journal.pone.0300892.g002>

with the significant reduction of eosinophils we observed in the colons of Rorc^{-/-} x TRAG mice compared to TRAG mice. Despite this significant reduction in eosinophils, Rorc^{-/-} x TRAG mice do not show improved immune profiles of other inflammatory cells or amelioration of

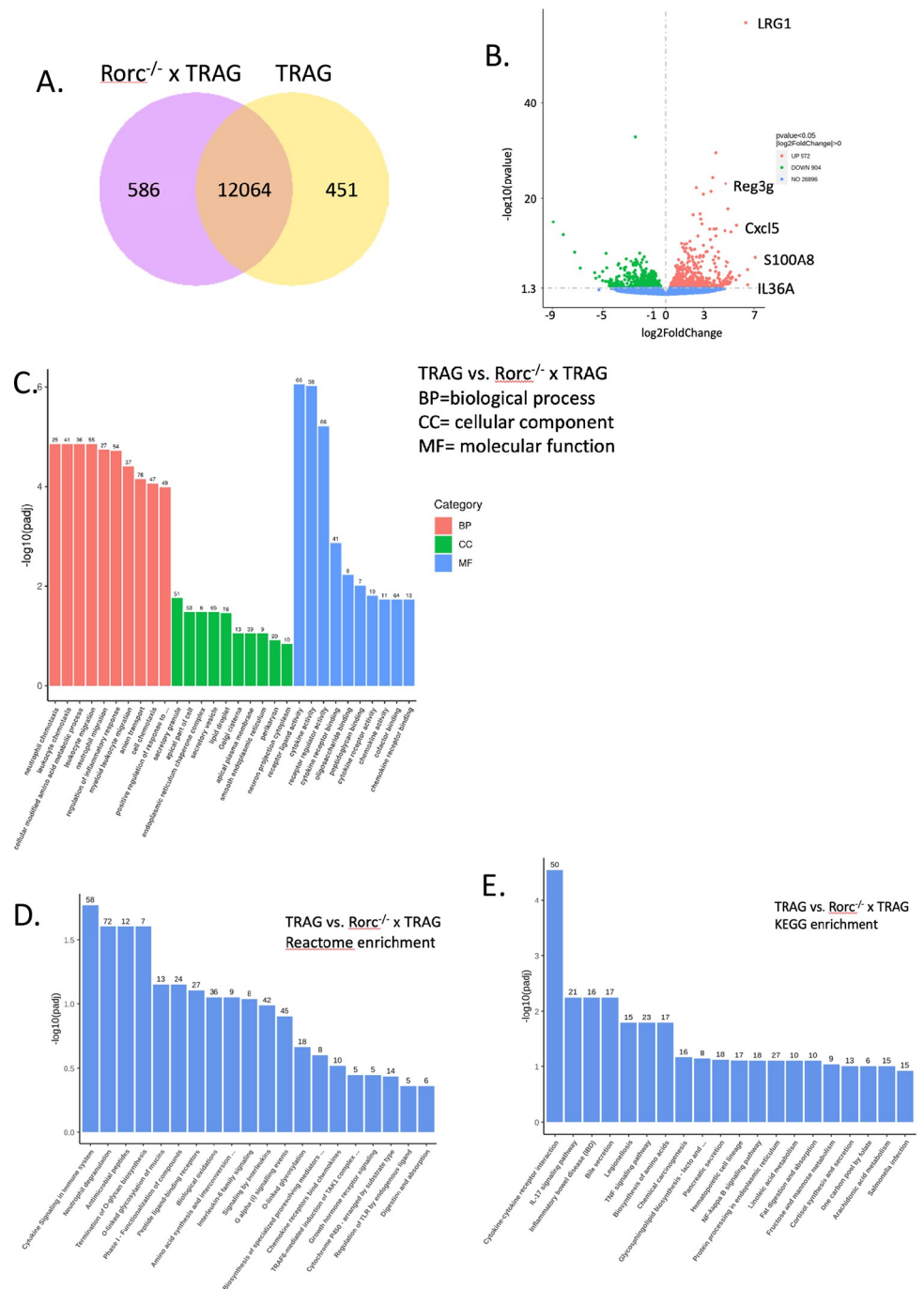


Fig 3. RNA profiles of TRAG and *Rorc*^{-/-} x TRAG colonic mucosa. (A) Venn diagram of shared and unique transcripts. (B) Volcano plot of RNA with increased and decreased expression in TRAG vs. *Rorc*^{-/-} x TRAG colonic mucosa. (C) GO (D) KEGG and (E) Reactome enrichment analysis of TRAG vs. *Rorc*^{-/-} x TRAG colon mucosa.

<https://doi.org/10.1371/journal.pone.0300892.g003>

their colitis. Thus, eosinophils numbers are reduced but this does not ameliorate colitis in TRAG mice lacking RoRyt.

ILC3 derived IL17 and IL22 are also protective cytokines that promote antimicrobial gene expression, the latter through IL22R-induced STAT3 signaling [21–24]. Consistent with this, reactome enrichment analysis of TRAG vs. *Rorc*^{-/-} x TRAG mice identified antimicrobial

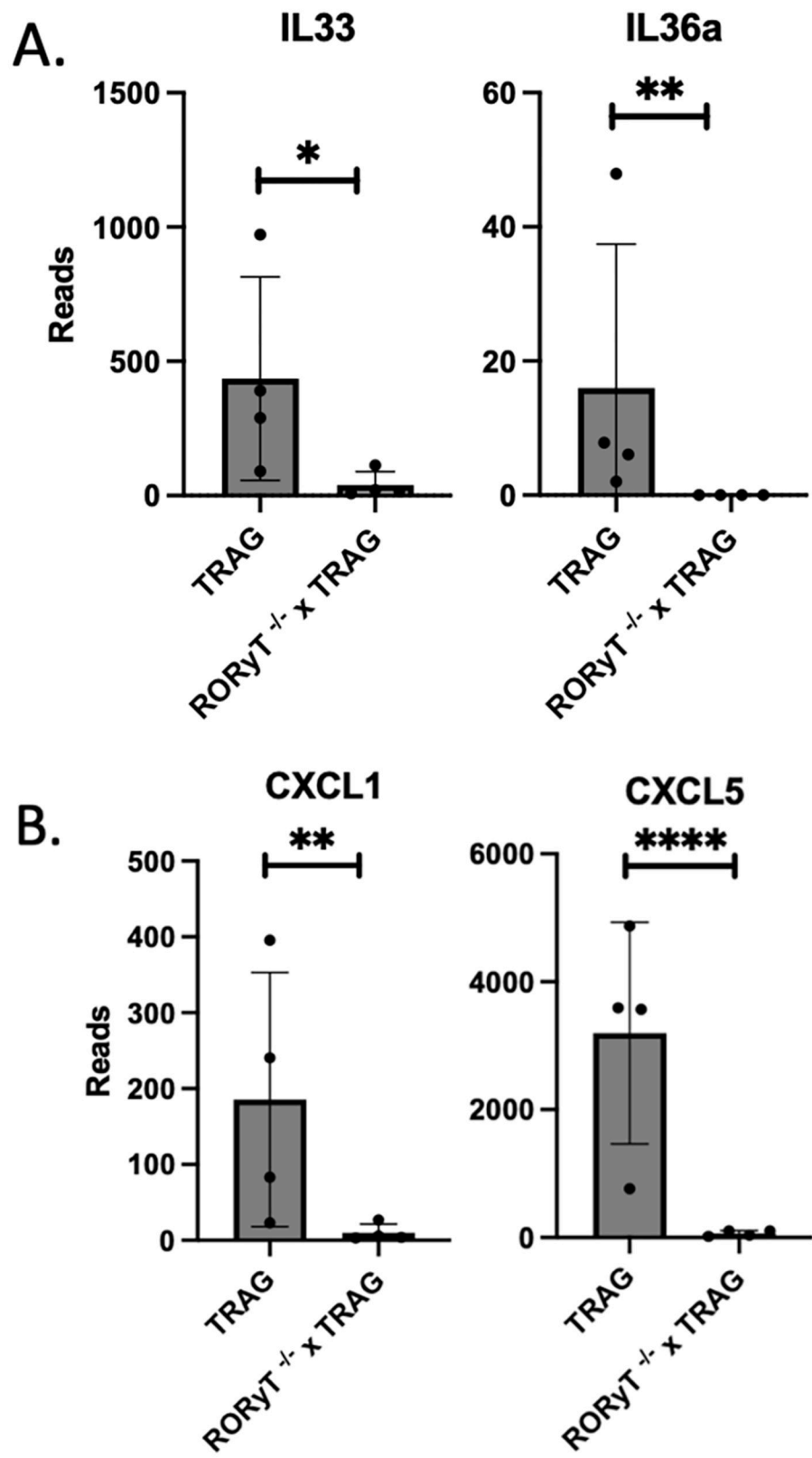


Fig 4. Reduced expression of cytokines that (A) induce eosinophilia and (B) are made by eosinophils in the colon mucosa of Rorc^{-/-} x TRAG vs. TRAG mice. * $p < 0.05$, ** $p < 0.01$, *** $p < 0.001$.

<https://doi.org/10.1371/journal.pone.0300892.g004>

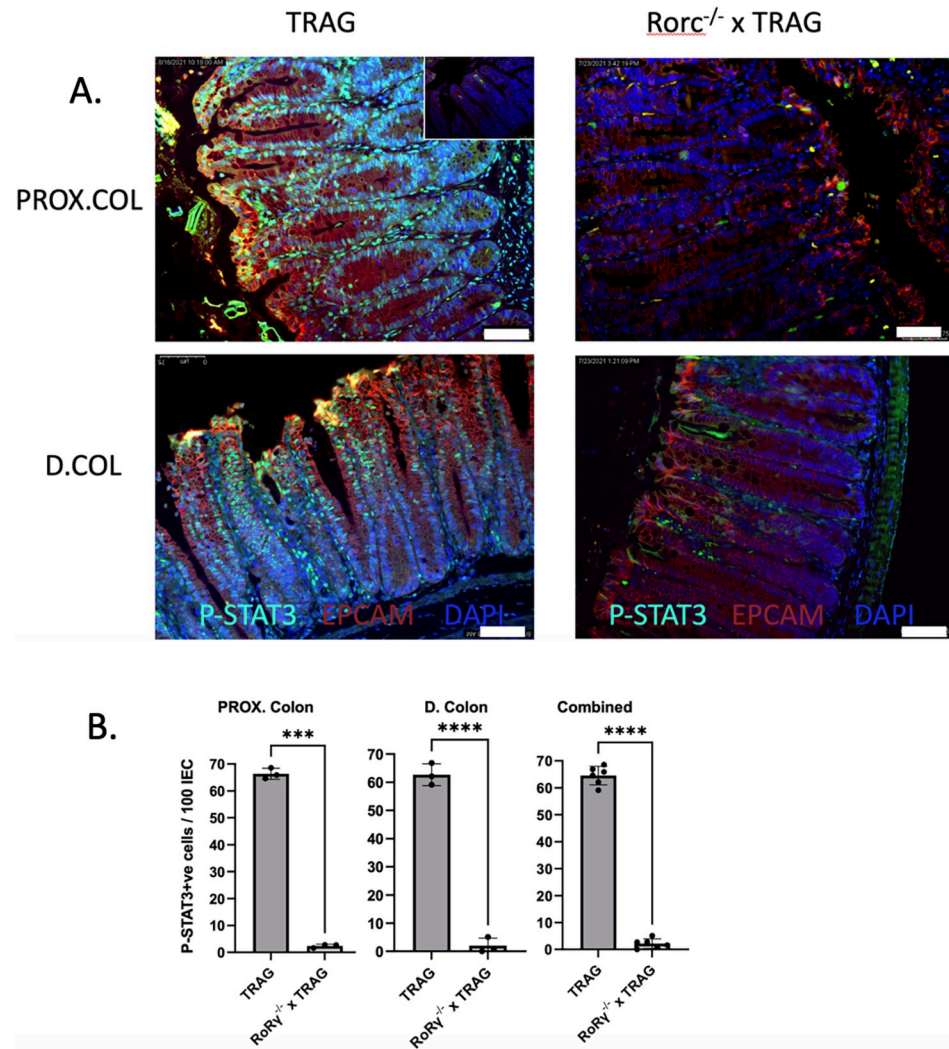


Fig 5. Reduced activation of STAT3 in TRAG mice lacking RoR γ t. (A) Immunolocalization of phospho-STAT3 in nuclei of epithelial cells from the distal and proximal colon of TRAG mice vs. *Rorc*^{-/-} x TRAG mice. (inset, top right = no primary control). Scale bar = 75 μ M. (B) Quantification of phospho-STAT3 positive IEC in TRAG vs. *Rorc*^{-/-} x TRAG colons showing the number of phospho-STAT3 cells per 100 epithelial cells in the proximal, distal and combined proximal+distal colons. n = 3. ***p<0.001, ****p<0.0001.

<https://doi.org/10.1371/journal.pone.0300892.g005>

peptides and IL-6 family signaling, which are STAT3 mediated pathways (Fig 3). IL22 produced by ILC3 drives STAT3 dependent antimicrobial gene expression that persists in *RAG1*^{-/-} small intestines after colonization with microbes [21]. We therefore examined STAT3 activation in TRAG vs. *Rorc*^{-/-} x TRAG colons. Consistent with observations in *RAG1*^{-/-} small intestine [21], intestinal epithelial cells of 8-week-old TRAG colons exhibited positive nuclear localization of phospho-STAT3, indicating that STAT3 was induced in these cells (Fig 5). *Rorc*^{-/-} x TRAG mice did not exhibit this pattern of phospho-STAT3 nuclear localization. These observations are consistent with the transcriptomic profile indicating reduced IL6 family cytokine signaling in *Rorc*^{-/-} x TRAG vs. TRAG mice, and consistent with prior reports indicating that ILC3-derived IL22 induces STAT3 in immunodeficient mice [21].

ILC3 derived IL22 induces phospho-STAT3 in intestinal epithelial cells resulting in transcription of antimicrobial genes [21]. We therefore examined the antimicrobial gene and

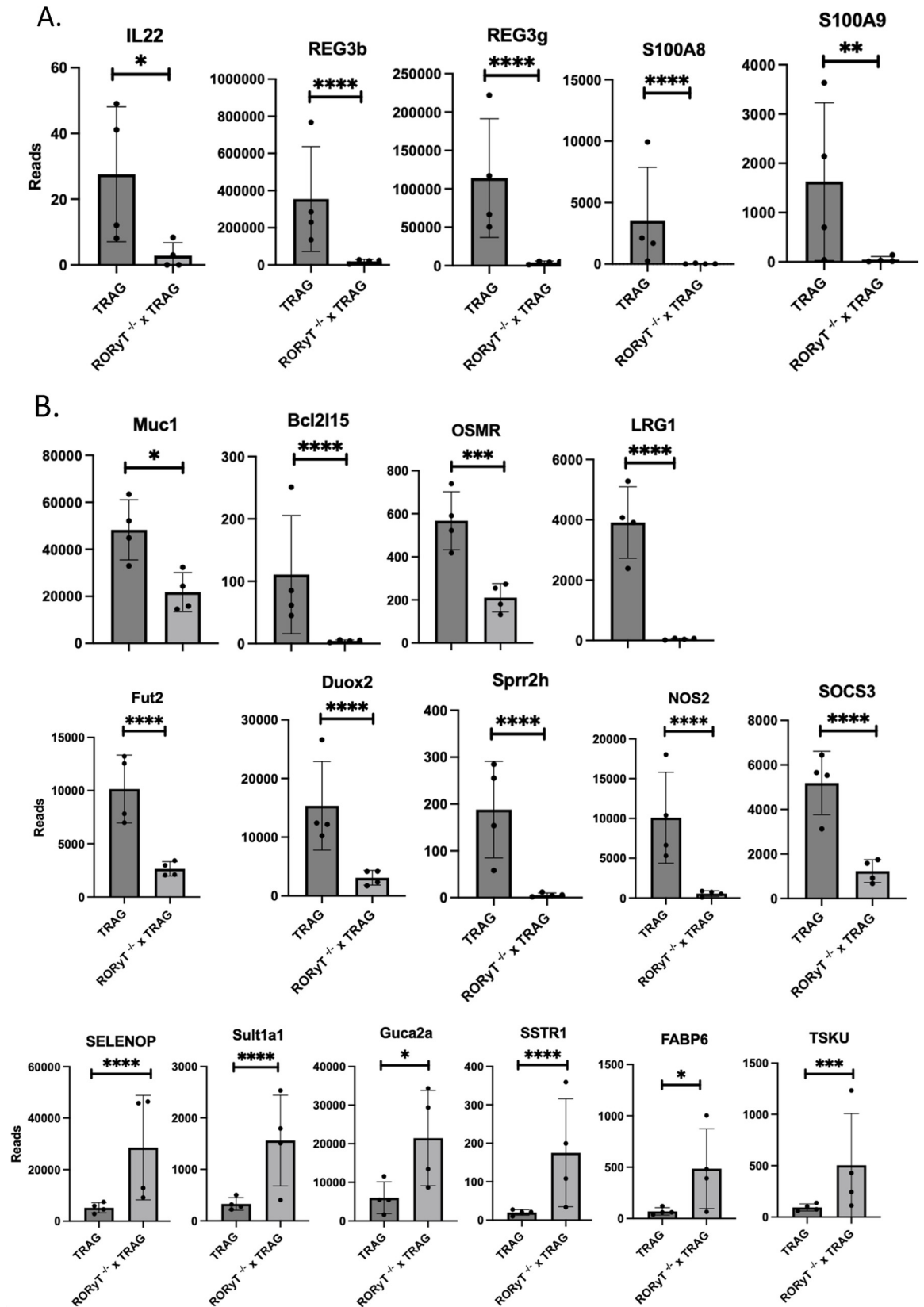


Fig 6. Gene expression changes in *Rorc*^{-/-} x TRAG vs TRAG colon mucosa. Decreased expression of (A) IL22 and antimicrobial factors, and (B) decreased expression of other IL22-induced genes. (C) Increased expression of mucosal repair related genes in the mucosa of *Rorc*^{-/-} x TRAG colon. Each data point represents one mouse. **p*<0.05, ***p*<0.01, ****p*<0.005, *****p*<0.001.

<https://doi.org/10.1371/journal.pone.0300892.g006>

STAT3 dependent transcripts in *Rorc*^{-/-} x TRAG vs. TRAG colonic mucosa. *Rorc*^{-/-} x TRAG colon mucosa expressed significantly less Reg3 β , Reg3 γ , S100A8 and S100A9, and less IL22 than TRAG colon mucosa (Fig 6). Other STAT3 induced genes known to be induced by IL22 in intestinal epithelial cells were also markedly reduced in *Rorc*^{-/-} x TRAG colons, including Muc1, Bcl2l15, OSMR, LRG1, Fut2, Duox2, Sprr2h, NOS2, and SOCS3 (Fig 6). Intestinal epithelial genes involved in mucosal repair or epithelial homeostasis that displayed increased expression in *Rorc*^{-/-} x TRAG mucosa vs. TRAG mucosa included SELENOP, Sult1a1, Guca2a, SSTR1, FABP6, and TSKU. Thus, the absence of RoR γ t leads to reduced expression of STAT3 dependent genes and compensatory gene signature consistent with mucosal repair. Many of the genes differentially regulated in the TRAG vs. *Rorc*^{-/-} x TRAG mice have been implicated in human IBD. For example, LRG1 the most markedly altered gene in *Rorc*^{-/-} x TRAG mucosa, is a signature serum marker for active ulcerative colitis and mucosal healing [25–27]. Polymorphisms in Fut2 resulting in non-secreter status are associated with risk for CD [28]. The OSM/OSMR pathway predicts response to anti-TNF therapy in patients with IBD [29]. It is clear that these and other differentially induced genes in *Rorc*^{-/-} x TRAG mice play important roles in innate immunity that should be considered to better understand IBD in immunocompetent settings.

The reduced expression of antimicrobial genes in *Rorc*^{-/-} x TRAG intestinal mucosa suggested that one reason *Rorc*^{-/-} x TRAG mice develop colitis may be due to microbes populating the gut. To test this, we treated 4-week-old *Rorc*^{-/-} x TRAG mice with antibiotics and assessed

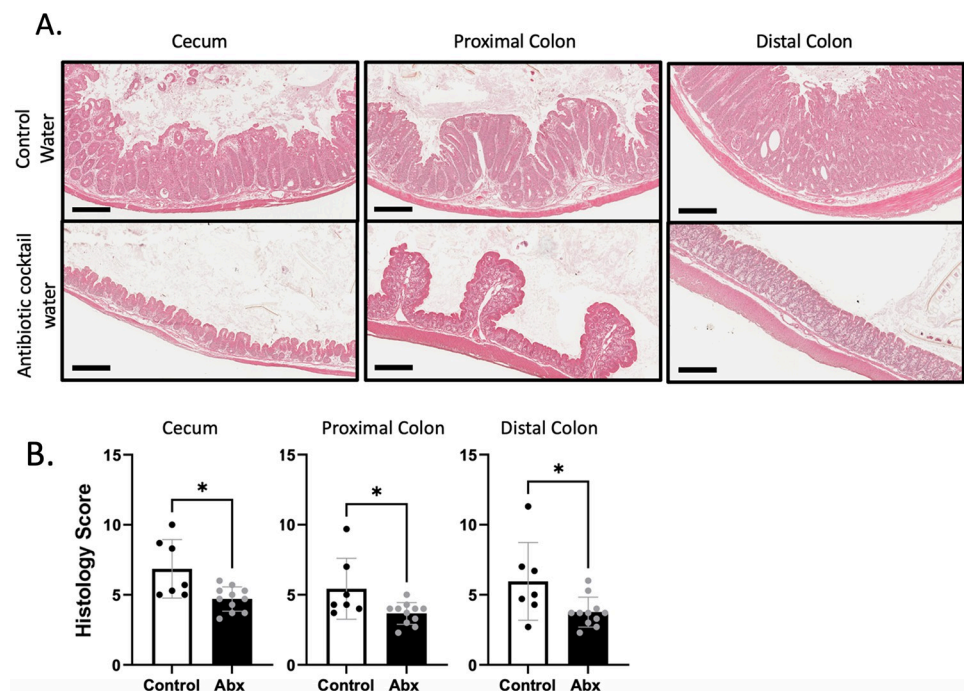


Fig 7. Amelioration of colitis in *Rorc*^{-/-} x TRAG mice treated with antibiotics. (A) Histological images of cecum, proximal colon and distal colon of 8-week-old *Rorc*^{-/-} x TRAG mice treated with control (grape KoolAid; upper panels) water or antibiotic cocktail water (lower panels) for 4 weeks. (B) Histological scores of tissues from *Rorc*^{-/-} x TRAG mice treated with control water or antibiotic cocktail (Abx). **p*<0.05.

<https://doi.org/10.1371/journal.pone.0300892.g007>

colitis at 8 weeks of age. Colitis was significantly attenuated by antibiotic treatment in the cecum, proximal colon, and distal colon of *Rorc*^{-/-} x TRAG mice (Fig 7). Thus, colitis in *Rorc*^{-/-} x TRAG mice is driven by microbes and can be prevented by administration of antibiotics. Together, these results reflect the dual nature of ILC3 in the intestine, promoting colitis by activating innate inflammation but preventing colitis by inducing antimicrobial responses through the IL22-STAT3 pathway in intestinal epithelial cells.

Discussion

Our results indicate that RoRyt contributes to inflammation and innate immune colitis in TRAG mice primarily in the distal colon. RoRyt is especially important for elevated numbers of eosinophils and, to a lesser extent neutrophils and ILCs in the intestinal mucosa of TRAG mice. Eosinophils, and not neutrophils, driven by the IL23-GMCSF axis have been implicated in colitis in both the T cell transfer and the *H. hepaticus* + anti-IL10R models of IBD [30]. The eosinophil driven colitis in those models exhibited increased expression of mucosal GMCSF, eotaxin, and RANTES but not IL5 [30]. We did not observe changes in expression of any of these cytokines between TRAG and *Rorc*^{-/-} x TRAG mice, despite significant decreases in eosinophils in the latter. This may be due to the fact that IL5 and GMCSF are predominantly T cell derived cytokines and the TRAG model lacks all adaptive immunity. However, ILC3 cells, which are absent in *Rorc*^{-/-} x TRAG mice, are critical for the production of GMCSF driven eosinophilia and innate colitis in the anti-CD40 or *H. hepaticus* infection of *RAG*^{-/-}, which are also innate models of IBD [31]. It is possible that a lack of ILC3 derived GMCSF accounts for the reduced eosinophilia we observed in *Rorc*^{-/-} x TRAG colon mucosa. Despite the reduction of eosinophilia the innate colitis persisted in *Rorc*^{-/-} x TRAG mice, unlike the reduced colitis observed in other innate models following suppression of eosinophilia [30]. There was also a significant decrease in expression of IL33, IL36a and IL36g in *Rorc*^{-/-} x TRAG mucosa, and these cytokines can induce eosinophil accumulation/activation [16, 17, 19], but these cytokines are not considered RoRyt or ILC3 dependent. Another explanation for reduced eosinophils in the mucosa of *Rorc*^{-/-} x TRAG mice may be that RoRyt plays a direct role in the function of eosinophils. Expression of RoRyt leading to IL17 production by eosinophils has been reported for eosinophils that accumulate in the lungs in models of acute and allergic aspergillosis [32]. Whether RoRyt plays a similar role in gut eosinophils remains to be determined. Our data indicate that eosinophil accumulation, but not colitis, are dependent on RoRyt in TRAG mice suggesting that eosinophil-independent and RoRyt-independent mechanisms drive the colitis in TRAG mice.

RoRyt is critical for the development of ILC3, which have been implicated as drivers of innate models of IBD [5, 33]. Despite this, RoRyt is largely dispensable for innate colitis in TRAG mice. This may represent the dual nature of ILC3 having both proinflammatory and antimicrobial roles in the intestine [34]. ILC3 produce IL22 which is a key cytokine for activation of epithelial cell STAT3 and induction of antimicrobial responses [21]. Indeed, *Rorc*^{-/-} x TRAG mice displayed significant reductions in pSTAT3 in the intestinal epithelium along with reduced expression of multiple antimicrobial factors including Reg3 β , Reg3 γ and calprotectin (S100A8 and S100A9). The reduction of these antimicrobial defenses may contribute to the colitis in *Rorc*^{-/-} x TRAG mice, as antibiotic treatment was able to reduce colitis in these mice. Reg3 γ is especially important for controlling gram positive microbes, while calprotectin has broader effects mediated by metal sequestration [35, 36]. The suppression of these two important antimicrobial factors in *Rorc*^{-/-} x TRAG mice is likely to allow a broad array of intestinal microbes and pathobionts to contact the mucosa of *Rorc*^{-/-} x TRAG mice leading to exacerbation of colitis. This microbial driven inflammation may also be exacerbated by

expression of TNFAIP3 in IEC which is permissive for invasion of the inner mucus layer of the colon by Actinobacteria and Gammaproteobacteria [7, 8].

In addition to the development of ILC3, RoRyt regulates the expression of IL23R and thus responsiveness of intestinal ILC3 to IL23 [33]. In the anti-CD40 antibody and *H. hepaticus* induced models of innate colitis, RoRyt-dependent ILC3 are required for development of colitis [5]. Although we observed some attenuation of colitis in the distal colon of *Rorc*^{-/-} x TRAG mice, the colitis was more severe compared to *RAG1*^{-/-} distal colons. In addition, there was no significant reduction in colitis severity in the cecum or proximal colon of *Rorc*^{-/-} x TRAG mice compared to TRAG mice. The innate colitis in anti-CD40 or *H. hepaticus* treated mice is acute and systemic, whereas the colitis in TRAG mice is chronic and limited to the colon. The systemic inflammation in these other models of innate colitis is driven by IL12, whereas the mucosal inflammation is driven by IL23 [37]. The persistence of colitis in *Rorc*^{-/-} x TRAG mice in the absence of systemic inflammation and the absence of ILC3 suggests that colitis in TRAG mice is driven by cytokines other than IL12 or IL23. The cellular mechanism of *H. hepaticus* induced innate colitis is not known, but anti-CD40 induces innate colitis by activating CD40 expressing antigen presenting cells (primarily dendritic cells) and can occur in germ-free mice [37]. Whether TRAG or *Rorc*^{-/-} x TRAG mice develop colitis in germ free conditions is not known, but the colitis in TRAG or *Rorc*^{-/-} x TRAG mice is prevented by antibiotics suggesting that microbes are required for colitis in this model [6]. Thus, the chronic, spontaneous, innate colitis of TRAG mice is distinct from the colitis observed in other innate models and this is also reflected in the RoRyt-independent colitis of this model.

Although the effects of RoRyt deletion are likely due to the loss of ILC3 in *Rorc*^{-/-} x TRAG mice, it should be noted that RoRyt plays roles in other cell types. A subset of neutrophils expresses RoRyt and rapidly produces IL17 in response to IL6 and IL23 [38]. These neutrophils are not dependent on RoRyt for development but play roles in responses to fungal pathogens and in inflammatory diseases. Whether RoRyt^{+ve} neutrophils play a role in IBD is not known. Additionally, RoRyt^{+ve} AIRE^{+ve} antigen presenting cells distinct from ILC3 have been described [33, 39]. These cells promote T cell responses to *Candida* but they are not typically found in the intestine [33]. Since the *Rorc*^{-/-} x TRAG model has no antigen receptor bearing cells, it is unlikely that these RoRyt^{+ve} APCs contribute to the innate inflammation in this model of colitis.

We observed a gene signature in *Rorc*^{-/-} x TRAG intestine consistent with epithelial cell injury and repair. There was increased expression in *Rorc*^{-/-} x TRAG mucosa, compared to TRAG mucosa, of SELENOP, TSKU, Sult1a1 and Guca2a, which are signatures of wound healing or intestinal epithelial responses to damage and are potential biomarkers of CD and UC [40–44]. Both IL17 and IL22 promote epithelial cell integrity and repair and the loss of RoRyt^{+ve} ILC3, a major source of IL17 and IL22 in the gut, likely leads to increased intestinal damage and the compensatory induction of these wound response pathways.

It is well known that RoRyt ILC3 cells have the potential to contribute to both colitis and prevention of colitis (Fig 8). Cytokines produced by ILC3, like IL17 and GM-CSF can drive innate immune cell recruitment and activation in the colon, while others, including IL17 and IL22 induce protective responses by activating mucosal repair and antimicrobial defenses. Our data suggests that in the colon, where a large burden of microbes is the normal state, the dominant function of ILC3 is likely to protect against microbially induced inflammation and colitis (Fig 8). RoRyt, or genes regulated by RoRyt, are promising targets for therapy but results from this study suggest that other RoRyt-independent mechanisms can contribute to innate immune mediated colitis. Thus, future efforts to identify RoRyt-independent mechanisms that contribute to innate immune mediated colitis will provide important additional information to help guide therapies to control innate immune inflammation in IBD.

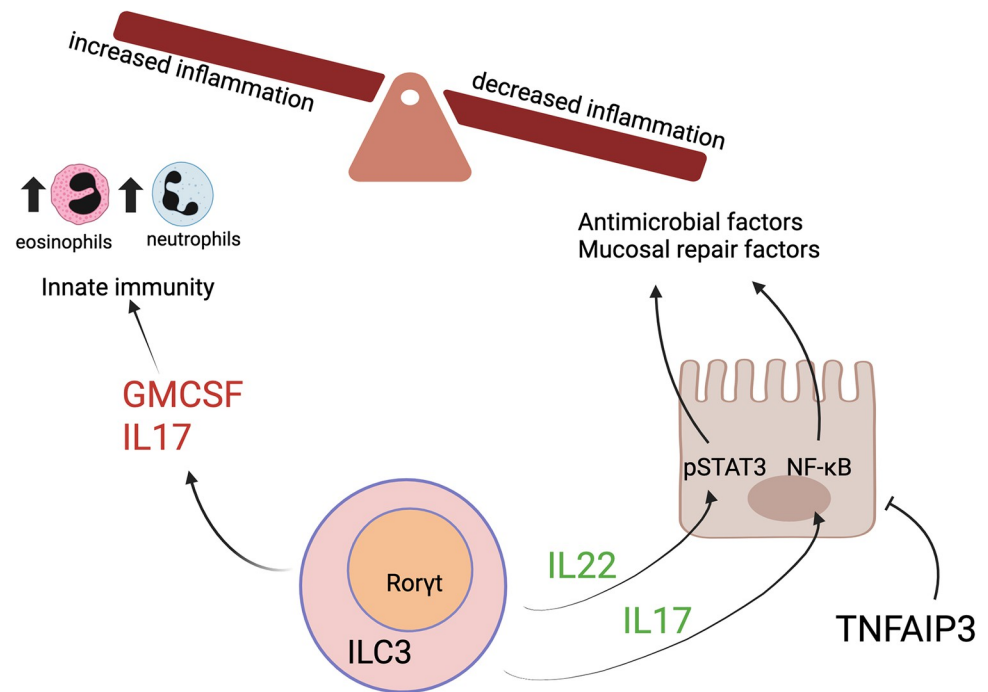


Fig 8. The dual nature of Roryt in colitis. Roryt-dependent ILC3 produce cytokines like IL17 and GM-CSF that drive innate immune mediated inflammation. Cytokines like IL22 and IL17 also reduce inflammation in the gut, by inducing mucosal healing and antimicrobial defenses. In the absence of Roryt-dependent ILC3, some innate immune mediated inflammation, especially eosinophilia, is reduced, but on balance the loss of mucosal defense roles of ILC3 leads to microbially driven, Roryt-independent colitis. Created with [Biorender.com](https://biorender.com).

<https://doi.org/10.1371/journal.pone.0300892.g008>

Supporting information

S1 File.
(XLSX)

Author Contributions

Conceptualization: Alvaro Torres-Huerta, Katelyn Ruley-Haase, Theodore Reed, David L. Boone.

Data curation: Theodore Reed.

Funding acquisition: David L. Boone.

Investigation: Alvaro Torres-Huerta, Katelyn Ruley-Haase, Theodore Reed, Antonia Boger-May, Derek Rubadeux, Lauren Mayer, Arpitha Mysore Rajashekara, Morgan Hiller, Madeleine Frech, Connor Roncagli, Cameron Pedersen, Mary Catherine Camacho, Lauren Hollmer, Lauren English, Grace Kane.

Methodology: Alvaro Torres-Huerta.

Supervision: David L. Boone.

Writing – original draft: Katelyn Ruley-Haase, David L. Boone.

Writing – review & editing: Alvaro Torres-Huerta, Katelyn Ruley-Haase, Theodore Reed, David L. Boone.

References

1. Kostic AD, Xavier RJ, Gevers D. The microbiome in inflammatory bowel disease: current status and the future ahead. *Gastroenterology*. 2014; 146(6):1489–99. Epub 20140219. <https://doi.org/10.1053/j.gastro.2014.02.009> PMID: 24560869; PubMed Central PMCID: PMC4034132.
2. McGovern DP, Kugathasan S, Cho JH. Genetics of Inflammatory Bowel Diseases. *Gastroenterology*. 2015; 149(5):1163–76.e2. Epub 20150807. <https://doi.org/10.1053/j.gastro.2015.08.001> PMID: 26255561; PubMed Central PMCID: PMC4915781.
3. Abraham C, Medzhitov R. Interactions between the host innate immune system and microbes in inflammatory bowel disease. *Gastroenterology*. 2011; 140(6):1729–37. <https://doi.org/10.1053/j.gastro.2011.02.012> PMID: 21530739; PubMed Central PMCID: PMC4007055.
4. Garrett WS, Lord GM, Punit S, Lugo-Villarino G, Mazmanian SK, Ito S, et al. Communicable ulcerative colitis induced by T-bet deficiency in the innate immune system. *Cell*. 2007; 131(1):33–45. <https://doi.org/10.1016/j.cell.2007.08.017> PMID: 17923086; PubMed Central PMCID: PMC2169385.
5. Buonocore S, Ahern PP, Uhlig HH, Ivanov II, Littman DR, Maloy KJ, et al. Innate lymphoid cells drive interleukin-23-dependent innate intestinal pathology. *Nature*. 2010; 464(7293):1371–5. <https://doi.org/10.1038/nature08949> PMID: 20393462; PubMed Central PMCID: PMC3796764.
6. Overstreet AM, LaTorre DL, Abernathy-Close L, Murphy SF, Rhee L, Boger AM, et al. The JAK inhibitor ruxolitinib reduces inflammation in an ILC3-independent model of innate immune colitis. *Mucosal Immunol*. 2018; 11(5):1454–65. Epub 20180709. <https://doi.org/10.1038/s41385-018-0051-2> PMID: 29988117; PubMed Central PMCID: PMC6162142.
7. Boger-May A, Reed T, LaTorre D, Ruley-Haase K, Hoffman H, English L, et al. Altered microbial biogeography in an innate model of colitis. *Gut Microbes*. 2022; 14(1):2123677. <https://doi.org/10.1080/19490976.2022.2123677> PMID: 36162004; PubMed Central PMCID: PMC9519015.
8. Murphy SF, Rhee L, Grimm WA, Weber CR, Messer JS, Lodolce JP, et al. Intestinal epithelial expression of TNFAIP3 results in microbial invasion of the inner mucus layer and induces colitis in IL-10-deficient mice. *Am J Physiol Gastrointest Liver Physiol*. 2014; 307(9):G871–82. Epub 20140918. <https://doi.org/10.1152/ajpgi.00020.2014> PMID: 25234043; PubMed Central PMCID: PMC4216993.
9. Kolodziej LE, Lodolce JP, Chang JE, Schneider JR, Grimm WA, Bartulis SJ, et al. TNFAIP3 maintains intestinal barrier function and supports epithelial cell tight junctions. *PLoS One*. 2011; 6(10):e26352. Epub 20111021. <https://doi.org/10.1371/journal.pone.0026352> PMID: 22031828; PubMed Central PMCID: PMC3198775.
10. Koelink PJ, Wildenberg ME, Stitt LW, Feagan BG, Koldijk M, van 't Wout AB, et al. Development of Reliable, Valid and Responsive Scoring Systems for Endoscopy and Histology in Animal Models for Inflammatory Bowel Disease. *J Crohns Colitis*. 2018; 12(7):794–803. <https://doi.org/10.1093/ecco-jcc/jiy035> PMID: 29608662; PubMed Central PMCID: PMC6022651.
11. Sheridan BS, Lefrançois L. Isolation of mouse lymphocytes from small intestine tissues. *Curr Protoc Immunol*. 2012; Chapter 3:3.19.1–3.1. <https://doi.org/10.1002/0471142735.im0319s99> PMID: 23129154; PubMed Central PMCID: PMC8128104.
12. Becht E, McInnes L, Healy J, Dutertre CA, Kwok IWH, Ng LG, et al. Dimensionality reduction for visualizing single-cell data using UMAP. *Nat Biotechnol*. 2018. Epub 20181203. <https://doi.org/10.1038/nbt.4314> PMID: 30531897.
13. Vivier E, Artis D, Colonna M, Diefenbach A, Di Santo JP, Eberl G, et al. Innate Lymphoid Cells: 10 Years On. *Cell*. 2018; 174(5):1054–66. <https://doi.org/10.1016/j.cell.2018.07.017> PMID: 30142344.
14. Murdock BJ, Falkowski NR, Shreiner AB, Sadighi Akha AA, McDonald RA, White ES, et al. Interleukin-17 drives pulmonary eosinophilia following repeated exposure to *Aspergillus fumigatus* conidia. *Infect Immun*. 2012; 80(4):1424–36. Epub 20120117. <https://doi.org/10.1128/IAI.05529-11> PMID: 22252873; PubMed Central PMCID: PMC3318426.
15. Kolls JK, Lindén A. Interleukin-17 family members and inflammation. *Immunity*. 2004; 21(4):467–76. <https://doi.org/10.1016/j.immuni.2004.08.018> PMID: 15485625.
16. Gurtner A, Borrelli C, Gonzalez-Perez I, Bach K, Acar IE, Núñez NG, et al. Active eosinophils regulate host defence and immune responses in colitis. *Nature*. 2023; 615(7950):151–7. Epub 20221212. <https://doi.org/10.1038/s41586-022-05628-7> PMID: 36509106; PubMed Central PMCID: PMC9977678.
17. De Salvo C, Wang XM, Pastorelli L, Mattioli B, Omenetti S, Buella KA, et al. IL-33 Drives Eosinophil Infiltration and Pathogenic Type 2 Helper T-Cell Immune Responses Leading to Chronic Experimental Ileitis. *Am J Pathol*. 2016; 186(4):885–98. Epub 20160222. <https://doi.org/10.1016/j.ajpath.2015.11.028> PMID: 26908008; PubMed Central PMCID: PMC5807926.

18. Queen D, Ediriweera C, Liu L. Function and Regulation of IL-36 Signaling in Inflammatory Diseases and Cancer Development. *Front Cell Dev Biol.* 2019; 7:317. Epub 20191204. <https://doi.org/10.3389/fcell.2019.00317> PMID: 31867327; PubMed Central PMCID: PMC6904269.
19. Leon G, Hussey S, Walsh PT. The Diverse Roles of the IL-36 Family in Gastrointestinal Inflammation and Resolution. *Inflamm Bowel Dis.* 2021; 27(3):440–50. <https://doi.org/10.1093/ibd/izaa232> PMID: 32860042.
20. Dolitzky A, Shapira G, Grisaru-Tal S, Hazut I, Avlas S, Gordon Y, et al. Transcriptional Profiling of Mouse Eosinophils Identifies Distinct Gene Signatures Following Cellular Activation. *Front Immunol.* 2021; 12:802839. Epub 20211214. <https://doi.org/10.3389/fimmu.2021.802839> PMID: 34970274; PubMed Central PMCID: PMC8712732.
21. Mao K, Baptista AP, Tamoutounour S, Zhuang L, Bouladoux N, Martins AJ, et al. Innate and adaptive lymphocytes sequentially shape the gut microbiota and lipid metabolism. *Nature.* 2018; 554(7691):255–9. Epub 20180122. <https://doi.org/10.1038/nature25437> PMID: 29364878.
22. Sonnenberg GF, Monticelli LA, Alenghat T, Fung TC, Hutnick NA, Kunisawa J, et al. Innate lymphoid cells promote anatomical containment of lymphoid-resident commensal bacteria. *Science.* 2012; 336(6086):1321–5. Epub 20120606. <https://doi.org/10.1126/science.1222551> PMID: 22674331; PubMed Central PMCID: PMC3659421.
23. Zenewicz LA, Yancopoulos GD, Valenzuela DM, Murphy AJ, Stevens S, Flavell RA. Innate and adaptive interleukin-22 protects mice from inflammatory bowel disease. *Immunity.* 2008; 29(6):947–57. <https://doi.org/10.1016/j.immuni.2008.11.003> PMID: 19100701; PubMed Central PMCID: PMC3269819.
24. Liang SC, Tan XY, Luxenberg DP, Karim R, Dunussi-Joannopoulos K, Collins M, et al. Interleukin (IL)-22 and IL-17 are coexpressed by Th17 cells and cooperatively enhance expression of antimicrobial peptides. *J Exp Med.* 2006; 203(10):2271–9. Epub 20060918. <https://doi.org/10.1084/jem.20061308> PMID: 16982811; PubMed Central PMCID: PMC2118116.
25. Serada S, Fujimoto M, Terabe F, Iijima H, Shinzaki S, Matsuzaki S, et al. Serum leucine-rich alpha-2 glycoprotein is a disease activity biomarker in ulcerative colitis. *Inflamm Bowel Dis.* 2012; 18(11):2169–79. Epub 20120228. <https://doi.org/10.1002/ibd.22936> PMID: 22374925.
26. Shinzaki S, Matsuoka K, Iijima H, Mizuno S, Serada S, Fujimoto M, et al. Leucine-rich Alpha-2 Glycoprotein is a Serum Biomarker of Mucosal Healing in Ulcerative Colitis. *J Crohns Colitis.* 2017; 11(1):84–91. Epub 20160727. <https://doi.org/10.1093/ecco-jcc/jjw132> PMID: 27466171; PubMed Central PMCID: PMC5175492.
27. Yasutomi E, Inokuchi T, Hiraoka S, Takei K, Igawa S, Yamamoto S, et al. Leucine-rich alpha-2 glycoprotein as a marker of mucosal healing in inflammatory bowel disease. *Sci Rep.* 2021; 11(1):11086. Epub 20210527. <https://doi.org/10.1038/s41598-021-90441-x> PMID: 34045529; PubMed Central PMCID: PMC8160157.
28. McGovern DP, Jones MR, Taylor KD, Marcianti K, Yan X, Dubinsky M, et al. Fucosyltransferase 2 (FUT2) non-secretor status is associated with Crohn's disease. *Hum Mol Genet.* 2010; 19(17):3468–76. Epub 20100622. <https://doi.org/10.1093/hmg/ddq248> PMID: 20570966; PubMed Central PMCID: PMC2916706.
29. West NR, Hegazy AN, Owens BMJ, Bullers SJ, Linggi B, Buonocore S, et al. Oncostatin M drives intestinal inflammation and predicts response to tumor necrosis factor-neutralizing therapy in patients with inflammatory bowel disease. *Nat Med.* 2017; 23(5):579–89. Epub 20170403. <https://doi.org/10.1038/nm.4307> PMID: 28368383; PubMed Central PMCID: PMC5420447.
30. Griseri T, Arnold IC, Pearson C, Krausgruber T, Schiering C, Franchini F, et al. Granulocyte Macrophage Colony-Stimulating Factor-Activated Eosinophils Promote Interleukin-23 Driven Chronic Colitis. *Immunity.* 2015; 43(1):187–99. <https://doi.org/10.1016/j.immuni.2015.07.008> PMID: 26200014; PubMed Central PMCID: PMC4518500.
31. Pearson C, Thornton EE, McKenzie B, Schaupp AL, Huskens N, Griseri T, et al. ILC3 GM-CSF production and mobilisation orchestrate acute intestinal inflammation. *Elife.* 2016; 5:e10066. Epub 20160118. <https://doi.org/10.7554/eLife.10066> PMID: 26780670; PubMed Central PMCID: PMC4733039.
32. Yadav B, Specht CA, Lee CK, Pokrovskii M, Huh JR, Littman DR, et al. Lung eosinophils elicited during allergic and acute aspergillosis express ROR γ t and IL-23R but do not require IL-23 for IL-17 production. *PLoS Pathog.* 2021; 17(8):e1009891. Epub 20210831. <https://doi.org/10.1371/journal.ppat.1009891> PMID: 34464425; PubMed Central PMCID: PMC8437264.
33. Abramson J, Dobeš J, Lyu M, Sonnenberg GF. The emerging family of ROR γ t. *Nat Rev Immunol.* 2023. Epub 20230721. <https://doi.org/10.1038/s41577-023-00906-5> PMID: 37479834.
34. Zeng B, Shi S, Ashworth G, Dong C, Liu J, Xing F. ILC3 function as a double-edged sword in inflammatory bowel diseases. *Cell Death Dis.* 2019; 10(4):315. Epub 20190408. <https://doi.org/10.1038/s41419-019-1540-2> PMID: 30962426; PubMed Central PMCID: PMC6453898.

35. Mukherjee S, Zheng H, Derebe MG, Callenberg KM, Partch CL, Rollins D, et al. Antibacterial membrane attack by a pore-forming intestinal C-type lectin. *Nature*. 2014; 505(7481):103–7. Epub 20131120. <https://doi.org/10.1038/nature12729> PMID: 24256734; PubMed Central PMCID: PMC4160023.
36. Zackular JP, Chazin WJ, Skaar EP. Nutritional Immunity: S100 Proteins at the Host-Pathogen Interface. *J Biol Chem*. 2015; 290(31):18991–8. Epub 20150608. <https://doi.org/10.1074/jbc.R115.645085> PMID: 26055713; PubMed Central PMCID: PMC4521021.
37. Uhlig HH, McKenzie BS, Hue S, Thompson C, Joyce-Shaikh B, Stepankova R, et al. Differential activity of IL-12 and IL-23 in mucosal and systemic innate immune pathology. *Immunity*. 2006; 25(2):309–18. <https://doi.org/10.1016/j.immuni.2006.05.017> PMID: 16919486.
38. Taylor PR, Roy S, Leal SM, Sun Y, Howell SJ, Cobb BA, et al. Activation of neutrophils by autocrine IL-17A-IL-17RC interactions during fungal infection is regulated by IL-6, IL-23, RORYt and dectin-2. *Nat Immunol*. 2014; 15(2):143–51. Epub 20131222. <https://doi.org/10.1038/ni.2797> PMID: 24362892; PubMed Central PMCID: PMC3972892.
39. Hepworth MR, Monticelli LA, Fung TC, Ziegler CG, Grunberg S, Sinha R, et al. Innate lymphoid cells regulate CD4+ T-cell responses to intestinal commensal bacteria. *Nature*. 2013; 498(7452):113–7. Epub 20130522. <https://doi.org/10.1038/nature12240> PMID: 23698371; PubMed Central PMCID: PMC3699860.
40. Short SP, Pilat JM, Barrett CW, Reddy VK, Haberman Y, Hendren JR, et al. Colonic Epithelial-Derived Selenoprotein P Is the Source for Antioxidant-Mediated Protection in Colitis-Associated Cancer. *Gastroenterology*. 2021; 160(5):1694–708.e3. Epub 20210101. <https://doi.org/10.1053/j.gastro.2020.12.059> PMID: 33388316; PubMed Central PMCID: PMC8035252.
41. Niimori D, Kawano R, Niimori-Kita K, Ihn H, Ohta K. Tsukushi is involved in the wound healing by regulating the expression of cytokines and growth factors. *J Cell Commun Signal*. 2014; 8(3):173–7. Epub 20140827. <https://doi.org/10.1007/s12079-014-0241-y> PMID: 25159578; PubMed Central PMCID: PMC4165825.
42. Zhao XH, Zhao P, Deng Z, Yang T, Qi YX, An LY, et al. Integrative analysis reveals marker genes for intestinal mucosa barrier repairing in clinical patients. *iScience*. 2023; 26(6):106831. Epub 20230506. <https://doi.org/10.1016/j.isci.2023.106831> PMID: 37250791; PubMed Central PMCID: PMC10212979.
43. Yau YY, Wasinger VC, Hirten RP, Chuang E, Huntsman M, Stylli J, et al. Current Trends in IBD-Development of Mucosal-Based Biomarkers and a Novel Minimally Invasive Recoverable Sampling System. *Inflamm Bowel Dis*. 2021; 27(Suppl 2):S17–S24. <https://doi.org/10.1093/ibd/izab179> PMID: 34791290; PubMed Central PMCID: PMC9214562.
44. Ikpa PT, Sleddens HF, Steinbrecher KA, Peppelenbosch MP, de Jonge HR, Smits R, et al. Guanylin and uroguanylin are produced by mouse intestinal epithelial cells of columnar and secretory lineage. *Histochem Cell Biol*. 2016; 146(4):445–55. Epub 20160531. <https://doi.org/10.1007/s00418-016-1453-4> PMID: 27246004; PubMed Central PMCID: PMC5037145.